Artificially stacked of two-dimensional atomic layers: towards new van der Waals solids

Guanhui Gao[1,2,Ⅱ], Wei Gao[3], E. Cannuccia[4,Ⅱ], Jaime Taha-Tijerina[1], Luis Balicas[5], Akshay Mathkar[1], T.N. Narayanan[1], Zhen Liu[1], Bipin K. Gupta[6], Juan Peng[7], Yansheng Yin[2,]*, Angel Rubio[4,] *, Pulickel M. Ajayan[1,] *

[1]Department of Mechanical Engineering & Materials Science, Rice University, Houston, Texas 77005, United States
[2]Institute of Materials Science and Engineering, Ocean University of China, Qingdao, China
[3] Department of Chemistry Rice University, Houston, Texas 77005, United States
[4] Nano-Bio Spectroscopy Group and ETSF Scientific Development Centre, Departamento de Física de Materiales, CFM-CSIC-UPV/EHU-MPC and DIPC, University of the Basque Country UPV/EHU, Av. Tolosa 72, E-20018 San Sebastián, Spain
[5] National High Magnetic Field Lab, Florida State University, USA
[6] Dr. K S Krishnan Road, New Delhi-110012, India
[7] School of Chemistry and Chemical Engineering Nanjing University, China
[Ⅱ] These authors contributed equally to this work.

Abstract

Strong in-plane bonding and weak Van der Waals inter-planar interactions characterize a large number of layered materials, as epitomized by graphite. The advent of graphene (G), individual layers from graphite, and atomic layers isolated from a few other van der Waals bonded layered compounds has enabled the ability to pick, place and stack atomic layers of arbitrary compositions and build unique layered materials, which would be otherwise impossible to synthesize via other known techniques. Here we demonstrate this concept for solids consisting of randomly stacked layers of graphene and hexagonal boron nitride (*h*-BN). Dispersions of exfoliated *h*-BN layers and graphene have been prepared by liquid phase exfoliation methods and mixed, in various concentrations, to create artificially stacked *h*-BN/G solids. These van der Waals stacked hybrid solid materials show interesting electrical, mechanical and optical properties distinctly different from their starting parent layers. From extensive first principle

calculations we identify i) a novel approach to control the dipole at the *h*-BN/G interface by properly sandwiching or sliding layers of *h*-BN and graphene, ii) a way to inject carriers in graphene upon UV excitations of the Frenkel – like exciton of the *h*-BN layer(s). Our combined approach could be used to create artificial materials, made from the van der Waals stacking of robust atomic layers of different layered solids with vastly different properties.

Keywords: hexagonal boron nitride (h-BN), graphene, exfoliation, band gap, ab-initio, interfaces, dipole, excitons.

There are several layered compounds, characterized by van der Waals forces between individual layers, such as graphite, h-BN, dichalcogenides etc. and the ability to extract individual layers from these solids have brought renewed interest in manipulating these materials [1-4]. Graphene (G), monolayer of graphite, has received enormous attention and has been formed by various techniques such as chemical exfoliation of graphite and vapor deposition[5-7]. Very recently, another layered compound, h-BN has also been exfoliated to obtain individual layers. There is ongoing work to produce individual layers of dichalcogenides such as MoS_2 and WS_2[8]. In effect, today it is possible to isolate individual atomic layers from materials that span broad range of properties. Electronically, graphene is semi-metallic, h-BN is an insulator and dichalcogenide layers have semi-conducting properties. With the availability of these isolated atomic layers of various compositions and properties, there appears to be a unique opportunity to build artificially stacked (van der Waals) structures from layers of differing compositions and build hybrid materials that has not yet been explored. Here we demonstrate this concept and build extended solids, using two of the above-mentioned atomic layers, namely graphene and h-BN. There have been a few previous attempts to fabricate graphene electronic devices on h-BN (considered as the best substrate for graphene) and hybridized in-plane atomic layers containing h-BN and

graphene. However, the synthetic method we report here can provide a generic approach to fabricate a variety of hybrid layered materials containing atomic layers of various compositions and properties. This detailed experimental analysis is further complemented with extensive first principle models that provide new microscopical insight allowing to identify the novel electro-mechanical properties steaming from these new hetero – stacked layers materials.

It is well known that solvents with high surface tension can be successfully used to exfoliate graphene and h-BN[8-11]. Several solvents such as N, N-dimethylformamide (DMF)[12], 1,2-dichloroethane(EDC)[13], poly (m-phenyl-enevinylene-co-2,5-dictoxy-p-phenylenevinylene)[14] have been reported for h-BN exfoliation. One may also exfoliate h-BN by using Octadecylamine (ODA), amine-terminated polyethyleneglycol (PEG), and Lewis-bases amine molecules with long lipophilic or hydrophilic chains [15]. However, these solvents are toxic and have a high boiling point, which makes it difficult to achieve to large scalable production. Here, we exfoliate bulk h-BN and graphite powders using common solvents to yield single, double, few-layered h-BN nanosheets and graphene and then reassemble these as hybrid h-BN/G layered solids (see Supplementary information S2 for more exfoliation details). According to the Hansen solubility theory[16], parameters such as polarity, H-bonding, the cohesive energy density among others, are related to the effectiveness of the exfoliation process. Among these, surface tension is a key parameter[10]. Different solvents with strong enough surface tension to overcome the van der Waals forces of h-BN have been tested, and isopropanol (IPA) was selected to isolate h-BN because it can be easily removed after exfoliation. In addition, it is easy to scale up the exfoliation process with IPA to generate high-quality layers of h-BN and graphene with yields of the order of 10 wt. %.

We can fabricate a hybrid film of h-BN and graphene nanosheets by mixing the exfoliated h-BN dispersion with that of graphene. In addition, different h-BN/G compositions in the film could be tuned by varying the volume ratio between each dispersion (see Supplementary S5), leading to a tunable band gap in the final hybrid films which may function well as semiconductors.[17-24] The proposed model for h-BN/G stacking hybrids could be clearly identified from detailed theoretical first-principles modeling. The stacking sequence is controlled by the interface dipole, which can be used to trigger the doping of a multilayer graphene and as a consequence of band gap opening. We believe that those h-BN and graphene nanosheets tend to stack alternately, offering a new hetero-structure that cannot be made by any other techniques.

The h-BN and graphene nanosheets constitute our building blocks to produce extended solids as they assemble both laterally and in stacked direction to produce freestanding films. In our experiments, stacking of mono- and multi-layered flakes was observed in low-resolution TEM images (Fig.1b and Supplementary Fig. S1, S2). The lateral sizes of the exfoliated nanosheets range from 500 nm to 800 nm. The FFT pattern shown in the inset of Fig. 3b indicates a 13° rotational angle between the two layers keeping the hexagonal symmetry of the network. The h-BN/G nanosheets have an interlayer spacing of 3.356Å (see table1 and calculation detail in Supplementary S9), in between that of h-BN and graphite. The TEM mapping test (see Fig.1f, g) provides clear evidence that h-BN stacks on graphene layer by layer. In order to identify the atomic composition of the hybrid h-BN/G sheet, electron energy-loss spectroscopy (EELS) was performed. Figure 1(h) depicts the characteristic K-shell ionized edges of B, C and N, corresponding to the edges at 189, 289 and 407eV, respectively[25-27]. The visible edges of B, N and C reveal the existence of one or more layers of graphene on top of h-BN (supplementary Fig.

S3). Therefore, the hybrid nanosheets are composed of both h-BN and graphene that are stacked alternately, but there is no long-range order along the thickness direction.

Further structural characterization is obtained by Raman spectroscopy perform with a 514.5 nm laser excitation. The pure *h*-BN signal is located at 1364 cm^{-1} (see Table1 and Fig.S7c) [28], whereas pure graphene shows a characteristic G-peak around 1581.3cm^{-1} representing the in-plane bond-stretching motion of pairs of C sp^2 atoms, E_{2g} mode. The 2D band is located at 2643.3 cm^{-1} and corresponds to sp^2 atomic vibration[29], and the D band at 1313.7 cm^{-1} indicates the graphene defect. For our new *h*-BN/G hybrids, the G peak is located at 1575 cm^{-1} and the 2D peak at 2661 cm^{-1}, with a broad band centered at 1325 cm^{-1}, probably due to the overlap of the D band of graphene and the 1365 cm^{-1} band in *h*-BN (supplementary Fig. S7). Raman mappings of *h*-BN/G flakes were performed at both 1580 cm^{-1} and 1370 cm^{-1}, showing the distribution of graphene and *h*-BN, with a size of 10μm×10μm (400 spectra in total). According to the mapping information, graphene is a top *h*-BN in the left region and *h*-BN is a top of graphene in the right region, as the arrows marked (Fig.2 a-b).

Thermal gravimetric analysis (TGA) showed a significant drop in mass starting at 678.9℃, which is attributed to the combustion of graphene sheets in air, and the same phenomena was observed on the hybrid (Fig. 2c), while *h*-BN is quite stable even beyond 800℃. From the TGA curve, the ratio of h-BN/graphene in this hybrid is calculated to be 3:1. We demonstrate a solution based self-assembling approach to achieve a layered solid hybrid of h-BN and graphene. This hybrid seems to be stable and forms small interlayer polar bonds to make the system stable. After characterizing structurally our new-stacked solid, we address the optical properties of this material. We first look at the ultraviolet-visible absorption spectrum shown in Fig. 2 d. The absorption edge of exfoliated h-BN is located at 236nm, which corresponds to an optical band

gap of 5.26 eV. Extended sheets of h-BN/G hybrid were produced by filtration of the mixed dispersions by varying the volume ratio between each material, leading to a tunable band gaps in the final h-BN/G hybrid (see Fig.2e and Supplementary S4 for the details on the calculations).

In Figures 3(a-c) we show the measured XPS spectra of B, N and C respectively from h-BN/G stacked solid. The main peak of the B 1s spectrum is at 190.1 eV corresponding to the B 1s in h-BN[33]. This indicates that B is mainly bonded to N, like in h-BN where three N atoms are surrounding one B atom. But there is a small shoulder peak around 189 eV, contributing to the broadening of the B 1s spectrum and which indicates a possible B_xC bonds in h-BN/G[34]. Polar covalent bonds between C atoms B atoms are possible due to their small difference in electronegativity[5]. This has been further confirmed by C1s spectrum and FT-IR (Fig.3d). N 1s spectrum is shown in figure b and it also proclaims that the main bonding is between B and N correnspondingto a peak at 398 eV. But a shoulder peak at higher energy (400.5 eV) is evidence from the spectrum and it indicates that N atoms partially bond with C atoms[5]. The C1s spectrum has a peak at 284.4 eV corresponding to that of graphene domains (indicated by C=C in spectrum) in h-BN/G. But it also has shoulder peaks at lower binding energy and higher binding energy. The peaks at lower binding energy indicates the presence of C-B bonds (in agreement with figure a) and the peak at higher binding energy shows the pres8ence of C-N bonds as evidence from figure 3b.

The attenuated total reflection Fourier transform infrared spectra (ATR-FTIR) of h-BN is shown Fig. 3d. It has two characteristic sharp features, one peak at 760 cm^{-1} indicative of in-plane bending vibration due to B-N, and another at ~1362 cm^{-1} that is characteristic of the out of plane vibration. In the h-BN/G hybrid, both peaks observed in the h-BN spectrum are observed, providing confirmation that the h-BN structure is undisturbed. An additional feature at 1101 cm^{-1}

is also observed, the FTIR spectrum of graphene shows a number of peaks, but no clear feature at 1101 cm^{-1}(see supplementary Fig. S5b). *Xu* et al.[35] attribute this peak to the icosahedral structure of B_4C while other studies[36] suggest the formation of boron carbide (B-C) bonds, resulting in IR absorption at 1100 cm^{-1}. While there is still a degree of uncertainty regarding the specifics of the chemical environment of the B-C bond, it is evident that there is chemical interaction between these stacked h-BN/G layers, which is resulting in the formation of amorphous BxC bonds, leading to the absorption feature at 1100 cm^{-1}.

Since graphene and *h*-BN have very different electronic properties, every combination of n *h*-BN/m-G layers sequence exhibits specific properties dictated by the stacking of graphene (and *h*-BN) layers at the *h*-BN/graphene interface and the number of *h*-BN and G layers.

In order to get more insight about the electronic properties of these new stacked structures, we performed extensive first principles density functional theory (DFT) simulations to determine their electronic and structural properties. Moreover, the optical response and the excited states have been computed using the state of the art of Many Body Perturbation theory based on the previously computed DFT ground-state wavefunctions and eigenvalues (see supplementary information S15 for the details of the calculations). We advance the main two points stemming from the calculations, i) those new structures open the possibility of mechanically controlling the electronic dipole at the *h*-BN/G interface and as consequence the electrostatic doping of the graphene surface; ii) we identify a new charge injection mechanism to provide carriers in graphene through the optical excitation of the *h*-BN by UV photons. We should mention that the calculations impose a commensurate configuration between the G and *h*-BN layers, this leads to the appearance of a small band gap (tenths of meV) in graphene as reported by other works [37],

however for the discussion below the presence of that small gap is irrelevant and, moreover, there is evidence that the incommensurability of the layers tends to wash-out that small gap opening[38]. The results presented here are in a different energy scale.

To illustrate the basic idea behind those new phenomena we first look at the possibility of having different interfacial dipoles and whether or not those can be controlled by the stacking sequence. We should mention that a similar idea was used[37] to dope graphene layers that are supported on a thin film of BN@Cu(111). First we want to address the question of whether we can have two different dipoles at two *h*-BN/G interfaces, if so we can have a distinct and different electrostatic doping of graphene via the insulating *h*-BN film. To asses this idea we designed a hetero structure sandwiching four layers of *h*-BN with graphene (see Fig. S13 (a), note that the results could be generalized to graphite@4-*h*-BN@graphene and other stacked configurations but to illustrate the physics it is best to look at this graphene@4 *h*-BN@graphene). Before discussing the results let us fix the notation presented schematically in Fig. 4 (c) by link-network diagrams. We have up to three different *h*-BN/G stacking sequences that mimic the AB and AA graphite stackings. Namely, AA stacking corresponds to an exact positioning of all C atoms on top on B and N atoms, this is indicated by full links between C, B and N atoms; AB stacking indicates the case where one C atom is above the center of the *h*-BN hexagon and the other on top of the nitrogen atom, that we denote as AB (nitrogen) or over the boron, denoted as AB (boron). In Fig 4 (a) we fix the left G/*h*-BN stacking to AB (boron) and look at the effect as a function of the different stacking sequence on the right interface *h*-BN/G. Changing the stacking sequence from AA to AB (nitrogen) changes the concentration of electrons at the interface, as it is shown in Fig. 4 (a), increasing or decreasing it with respect to the quasi symmetric configuration (AB (boron)

stacking at both the interfaces). This appears as a few meV change in the effective electrostatic potential change going through the heterostructure (see Fig. 4 (b) and Fig. S14 top panel in the supplementary materials). What we observe from the figure is that the interface between Graphene (G) and *h*-BN has an intrinsic dipole that comes from the work function mismatch and Pauli exchange repulsion that leads to interface charge rearrangement (see Fig. 4 (b)). One would expect this dipole to be equal on both G/*h*-BN interfaces, however as shown in Fig. 4 (a) this is not the case and it is a clear manifestation of the role of the crystallographic stacking sequence that is usually neglected. In fact this phenomena has been used previously[39] to tune the bandgap of trilayer graphene. This stacking-induced dipole asymmetry can be used to control the doping of the *h*-BN/G interface (on the right) through the length of the *h*-BN, without resorting to any external field. As the size of the *h*-BN buffer film increases, the electrostatic potential drops due to the different charges at both ends of *h*-BN, and moves the average effective potential acting on the second *h*-BN/G interface towards lower energies. This corresponds to an effective electron doping of the graphene, the amount of doping is linked to the length of the *h*-BN layer (see Fig. S14 (b) in supplementary materials). We should mention that the saturation is reached by increasing the number of *h*-BN layer, as shown here[37,]. We could even get hole doping for some specific arrangements. This idea can be extended to configurations in which instead of graphene we use a real noble metal like Cu or Au in order to induce a large variation of the dipoles and induced fields (and consequently of the doping level).

A second aspect of the same physical process discussed above would be the creation of an effective electric field though multilayer graphene. This has some nice implications for the case of trilayer graphene that, if grown in ABC stacking, exhibits a tunable gap by applying an electric field[39]. The simplified model to illustrate this idea consists of a trilayer graphene

sandwiched with *h*-BN (depicted in Fig. S13 (b)) such that we use different crystallographic stacking sequences at both ends to induce an asymmetric dipole and therefore an effective (small) field across. This is done in practice by changing the G/*h*-BN stacking sequence from AB (boron) to AB (nitrogen) or AA. The results plotted in Fig. 4 (e) show that the right effective potential can be either above or below the left one depending on the stacking.

The control of the dipole interface paves the way to several possible technological applications: the possibility to control the electrostatic doping and to convert mechanical energy into electrical one. A simple process of sliding the last layer induced a change in the potential and electrostatic doping. This effect depends on the underlying hybrid-stacked heterostructures.

After having discussed the change of the electronic properties induced by playing with the crystallographic stacking, we address now the optical properties. We know *h*-BN is characterized for having a strong Frenkel-like exciton around 6.1 eV and an onset of the absorption at about 5.8 eV[20,40] that is far from the main absorption region of graphene[41]. Then we expect interesting mixed excitonic states in our heterostructures. In fact, this is the case. The calculated optical absorption spectrum of a solid composed of alternated *h*-BN/G layers with ratio 1:1 and 3:1 is shown in Fig. 5 (a). The analysis of the excitonic wavefunctions reveals that in the 1:1 case each exciton in the 3-6 eV region is composed by electronic transitions from nitrogen to the *C*-*C* bond of graphene. The excitonic wavefunction for those main peaks is characterised by having the electron mainly localized on the graphene layer if the hole is on the N of the *h*-BN layer, as shown in Fig. 5 (b). The lower energy excitations are mainly localized on the graphene layer and have negligible contributions from the *h*-BN.

On the other hand in the 3:1 case the exciton at 6.11 eV is mainly localized on the *h*-BN layer, as Fig. 5 (c) shows. The excitons in the shadowed energy region drawn in Fig. 5 (a) have a pure character whereas the excitations below have a hybrid character. The presence of an exciton localized on the central *h*-BN layer in the 3:1 case is due to the fact that a larger number of *h*-BN layers reduces the metallic-like screening introduced by graphene when compared to the 1:1 case. In the limit of an infinite number of *h*-BN layers the position of the bound exciton approaches the *h*-BN bulk value of 6.1 eV[40] from below.

In the 1:1 case the screening exerted by graphene is higher causing a redistribution of the well defined unique excitonic peak of *h*-BN into several less intense excitons with a “mixed” nature. So the Frenkel nature of the *h*-BN exciton is modified and the exciton spreads over the surrounding graphene layers as Fig. 4(d) clearly shows. Those results open the possibility of using the BN-layers as optical active device in the UV that can inject charges in the carbon layers by the direct excitation of the exciton of the *h*-BN.

In conclusion, here we demonstrate a new synthetic approach towards building solid materials from stacking of atomic layers from layered structures having wide range of properties. Here such a solid is constructed from layers of conducting graphene and insulating h-BN. The chemical exfoliation technique and mixing approach we have used here results in random stacking of layers in both lateral and thickness directions. However, layer-by-layer deposition techniques could be used to build more ordered stacks although getting alternating stacking of monolayer over large thicknesses could be challenging. The concentration of each composition could be also tailored by using appropriate concentration of layers in the assembly; in our study we created h-BN/G films with varying concentrations of h-BN and G. The approach we have

reported here allows the creation of novel materials built from 2D building blocks through their van der Waals stacking to produce hybrid-layered materials. Such materials could have fascinating properties due to the large number of interfaces between electronically dissimilar, flat, atomic layers bound through weak van der Waals forces. In fact we have shown how the crystallographic stacking introduced a new order parameter that controls the interfacial dipoles and therefore the effective electrostatic doping of the surfaces.

Corresponding Author

Pulickel M. Ajayan: ajayan@rice.edu

Angel Rubio: angel.rubio@ehu.es

Yansheng Yin: ysyin@shmtu.edu

Acknowledgements

Financial support was provided by the European Research Council Advanced Grant DYNamo (ERC-2010-AdG -Proposal No. 267374), Spanish (FIS2011-65702-C02-01 and PIB2010US-00652), ACI-Promociona (ACI2009-1036), Grupos Consolidados UPV/EHU del Gobierno Vasco (IT-319-07) and computational time was granted by i2basque, SGIker Arina and BSC "Red Espanola de Supercomputacion".

References:

(1) A. K. Grim & K. S. Novosibirsk. The rise of graphene. *Nature Mater.* **2007**, 6, 183-191.

(2) Corso, M., Auwärter, W. et al. Boron nitride nanometer. *Science* **2004**, 303(5655), 217-220.

(3) A. Nagasaki, N. Teatime, Y. Gamow, T. Kasai, Kagoshima, C. Electronic structure of monolayer hexagonal boron nitride physicked on metal surfaces. *Phys. Rev. Letti.* **1995**, 75, 3918.

(4) D. Pacilé, J. C. Meyer et al. The two-dimensional phase of boron nitride: Few-atomic-layer sheets and suspended membranes. *Applied Physics Letti.* **2008**, 92, 133107.

(5) Livvie Ci, Li Song et al. Atomic layers of hybridized boron nitride and graphene domains. *Nature Mater*. **2010**, 9, 435-430.

(6) Li Song, Livvie Ci et al. Large scale growth and characterization of atomic hexagonal boron nitride layers. *Nona Letti.* **2010**, 10, 3209-3215.

(7) Z. Lou, L. Song, S. Chao, J. Huang, L. Ma, J. Hang, J. Lou, P. M. Ajayan. Direct growth of graphene/hexagonal boron nitride stacked layers. *Nona letter* **2011**, 11 (5), 2032–2037.

(8) Jonathan N. Coleman, Mustang Lotta et al. Two-dimensional nanosheets produced by liquid exfoliation of layered. *Science*. **2011**, 331, 568.

(9) S. Changeover, S. Biracial. Two-dimensional C/BN core/shell structures. *Physical Review B* **2011**, 83, 165448.

(10) Srivastava, A., Galande, C., et al. Novel liquid precursor-based facile synthesis of large-area continuous, single, and few-layer graphene films. *Chem. Mater*. **2010**, 22 (11), 3457–3461.

(11) A. Nag, K. Railroading, et al. Graphene analogues of BN: novel synthesis and properties. *ACS Nona.* **2010**, 4 (3), 1539–1544.

(12) Y Lin, Tiffany V. Williams et al. Soluble, exfoliated hexagonal boron nitride Nanoseconds. J. *Phys. Chem. Letti.* **2010**, 1, 277–283.

(13) Chunyi Zhi, Yoshio Bando et al. Large-scale fabrication of boron nitride nanosheets and their utilization in polymeric composites with improved thermal and mechanical properties. *Adv. Mater*. **2009**, 21, 2889–2893.

(14) Jamie H. Warner, Mark H. R Emmeline et al. Atomic resolution imaging and topography of boron nitride sheets produced by chemical exfoliation. *ACS anon*, **2010**, 4, 1299–1304.

(15) Wei-Qiang Han, Lijun Wu et al. Structure of chemically derived mono- and few atomic-layer boron nitride sheets. *Applied Physics Letti.* **2008**, 93, 223103.

(16) Y Lin, Tiffany V. Williams et al. Aqueous dispersions of few-layered and mono layered hexagonal boron nitride nanosheets from fornication-assisted hydrolysis: critical role of water. J. *Phys. Chem. C* **2011**, 115, 2679–2685.

(17) Xue J., Sanchez-Yamagishi J. et al. Scanning tunneling microscopy and spectroscopy of ultra flat graphene on hexagonal boron nitride. *Nat. Mater*. **2011**, 10 (4), 282–285.

(18) S. D. Begin Sun, Z. et al. Multi-component solubility parameters for single walled carbon nanometer-solvent mixtures. *ACS Nona* **2009**, 3, 2340-2350.

(19) C. R. Dean, A. F. Young et al. Boron nitride substrates for high-quality graphene electronics. *Nature biotechnology* 2010, 5, 722-726.

(20) Benji Watanabe, Latashia Tanisha, History Kaunda. Direct-band gap properties and evidence for ultraviolet lasing of hexagonal boron nitride single crystal. *Nature mater*. **2004**, 3, 404-409.

(21) Girt C. O., Meyer J. C. et al. Graphene at the edge: stability and dynamics. *Science* **2009**, 323, 1705–1708.

(22) J. Kotakoski, C. H. Jin et al. electron knock-on damage in hexagonal boron nitride monolayer. *Physical Review B* **2010**, 82, 113404.

(23) Churchgoing Jun, Fang Lin et al. Fabrication of a freestanding boron nitride single layer and its defect assignments. *Physical Review Letti.* **2009**, 102, 195505.

(24) Jannie C. Meyer, C. Malinowski et al. Direct imaging of lattice atoms and topological defects in graphene membranes. *Nona Letti.* **2010**, 10, 3209-3215.

(25) Meyer, J. C., Chuckling, A. et al. Selective sputtering and atomic resolution imaging of atomically thin boron nitride membranes. *Nona Letti.* **2009**, 9, 2683–2689.

(26) Nastily Elem, Rolf Erin et al. Atomically thin hexagonal boron nitride probed by ultrahigh-resolution transmission electron microscopy. *Physical Review B* **2009**, 80 155425.

(27) R. BN/G, M. Kodiak N. J. Zealous. High-angular-resolution electron energy loss spectroscopy of hexagonal boron nitride. *Applied Physics Letti.* **2007**, 90, 204105.

(28) Ludger Wirtz, Angel Rubio, Raul Arenal de la Concha and Annick Loiseau, *Ab initio* calculations of the lattice dynamics of boron nitride nanotubes, Phys. Rev. B **2003,** 68, 045425. R. Arenal, A. C. Ferrari, S. Reich, L. Wirtz, J.-Y. Mevellec, S. Lefrant, A. Rubio, and A. Loiseau Raman *Spectroscopy of Single-Wall Boron Nitride Nanotubes. Nona*

Letters **2006** 6 (8), 1812-1816 . Sergio Azevedo, J R Kaschny et al. A theoretical investigation of defects in a boron nitride monolayer. *Biotechnology* **2007**, 18, 495707.

(29) A. C. Ferrari, J. C. Meyer et al. Raman spectrum of graphene and graphene layers. *Physical Review Letti.* **2006**, 97, 187401.

(30) Sun, Z.; An, Z.; Tao, J.; Beetler, E.; Shu, Y.; Tour, J. M. Growth of graphene from solid carbon sources. *Nature* **2010**,468, 549–552.

(31) T. N. Narayanan, D. Sakthi Kumar, et al. Strain induced anomalous red shift in microscopic iron oxide prepared by a novel technique Bull. *Mater. Sci. 2008, 31, 759-766.*

(32) Y. Miyamoto, A. Rubio, Louie, Cohen. Electronic properties of tubule forms of hexagonal BC_3. *Phys. Rev. B* **1994**, 50, 18360.

(33) Wanda, Y.K Yap, M Yoshiko, Y Miro, T Kawasaki. The control of B-N and B-C bonds in BCN films synthesized using pulsed laser deposition. Diamond and Related materials **2010**, 9, 620-624.

(34) I. Carets, I. Jimenez, J.M. Alberta. BCN films with controlled composition obtained by the interaction between molecular beams of B and C with nitrogen ion beams. *Diamond and Related Materials* **2003**, 12, 1079–1083.

(35) Shulman XU, Xingu MA, Mingle SUN. Synthesis of boron carbonization films by plasma-based ion implantation. *Key Engineering Materials* **2007**, 353-358, 1850-1853.

(36) J. H. Chen, C. Jan, S.D. Xian, Mada Bigamist, Michael S. Fuhrer. Intrinsic and extrinsic performance limits of graphene devices on SiO_2. *Nature Biotechnology* **2008**, 3, 206-209.

(37) M. Bokdam, P.A. Khomyakov, G. Brocks, Z. Zhong, and P.J. Kelly. Electrostatic doping of graphene through ultrathin hexagonal boron nitride films. *Nano Lett.*, **2011**, 11 (11), pp 4631–4635

(38) C. R. Dean, A. F. Young, I.Meric, C. Lee, **L. Wang**, S. Sorgenfrei, K. Watanabe, T. Taniguchi, P. Kim, K. L. Shepard and J. Hone. Boron nitride substrates for high-quality graphene electronics. *Nat. Nanotechnol.* **2010**, 5, 722; J.Xue, J. Sanchez-Yamagishi, D. Bulmash, P. Jacquod, A. Deshpande, K. Watanabe, T. Taniguchi, P. Jarillo-Herrero and B. J. LeRoy. Scanning tunnelling microscopy and spectroscopy of ultra-flat graphene on hexagonal boron nitride. *Nat. Mater.* **2011**, 10, 282; Régis Decker, Yang Wang, Victor W.

Brar, William Regan, Hsin-Zon Tsai, Qiong Wu, William Gannett, Alex Zettl, and Michael F. Crommie. Local Electronic Properties of Graphene on a BN Substrate via Scanning Tunneling Microscopy. *Nano Lett.* **2011**, 11, 2291

(39) C. H. Lui, Z. Li, K.F. Mak, E. Cappellutti and T. F. Heinz, Observation of an electrically tunable band gap in trilayer graphene. *Nature Physics* **2011,** 7, 944–947

(40) L. Wirtz, A. Marini, A. Rubio Excitons in boron nitride nanotubes: dimensionality effects. *Phys. Rev. Lett.* **96**, 126104 (2006)

(41) P. Trevisanutto, M. Holzmann, M. Cote and V. Olevano Ab initio high-energy excitonic effects in graphite and graphene. *Phys. Rev. B* **2010** 81, 121405

Fig.1 a) h-BN and graphene hybrid nanosheets stack randomly. b) Low resolution TEM images of few-layer h-BN/graphene hybrid stacking prepared by mixing h-BN/IPA with graphene/DMF. c) High resolution TEM image of b) at the edge, the FFT in the inset reveals two layers stacking with a relative rotational angle of 13°. d) Individual atomic layers reconstructed by masking the FFT pattern from the area in image (c) (red line). e) Free-standing films of h-BN, BN/G hybrid,

graphene. f) The h-BN/GTEM image for mapping. g) Boron mapping of image (f) and yellow color is graphene nanosheets; blue color is exfoliated h-BN nanosheets. h) EELS spectrum of h-BN/graphene hybrid, K-shell excitations of B, C and N.

Materials	XRD e=1.5418 Å	Raman (cm^{-1}) D	G	2D
h-BN	2θ=26.74° d=3.334Å	1365		
Graphene	2θ=26.34° d=3.383Å	1313.7	1581.3	2643.3
h-BN/G	2θ=26.56° d=3.356Å	1325	1575	2661

Table 1 Properties of pure h-BN, graphene and hybrids of h-BN/G (1:1) respectively.

Fig. 2 Evidence for a hybrid structure composed of h-BN and graphene: a, b) Raman Mapping of G/BN flakes; a) Mapping at 1580 cm^{-1} and (b) 1370 cm^{-1}. c)) TGA spectrum of graphene, hybrid of h-BN/G, h-BN; d) UV-vis spectra of h-BN and hybrid of h-BN/graphene (3:1), respectively; e) Band gap of hybrid of h-BN/G by different ratio between h-BN and graphene.

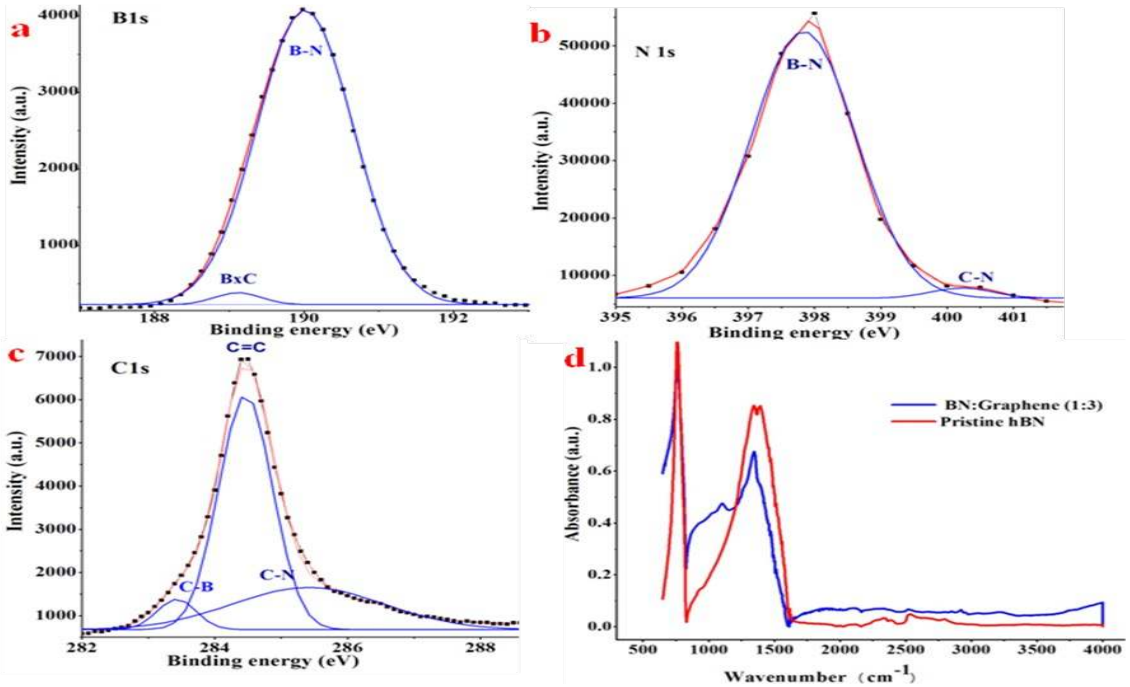

Fig. 3 Evidence for *h*-BN/C hybrid: a–c) XPS spectra of B, N and C 1*s* core levels, respectively. The spectrum curves (filled diamonds) are deconvolution (blue curves) by Gaussian fitting (red curves), indicating possible multi-bonding information; d) ATR-FTIR spectra of exfoliated h-BN and h-BN/G hybrid (1:3). Characteristic peaks at 760 cm^{-1} and 1362 cm^{-1} corresponding to in-plane and out of plane are observed in the h-BN spectrum (red). In the hybrid h-BN/G spectrum, a feature at ~1101 cm^{-1} is observed in addition to the peaks at 760 cm^{-1} and 1360

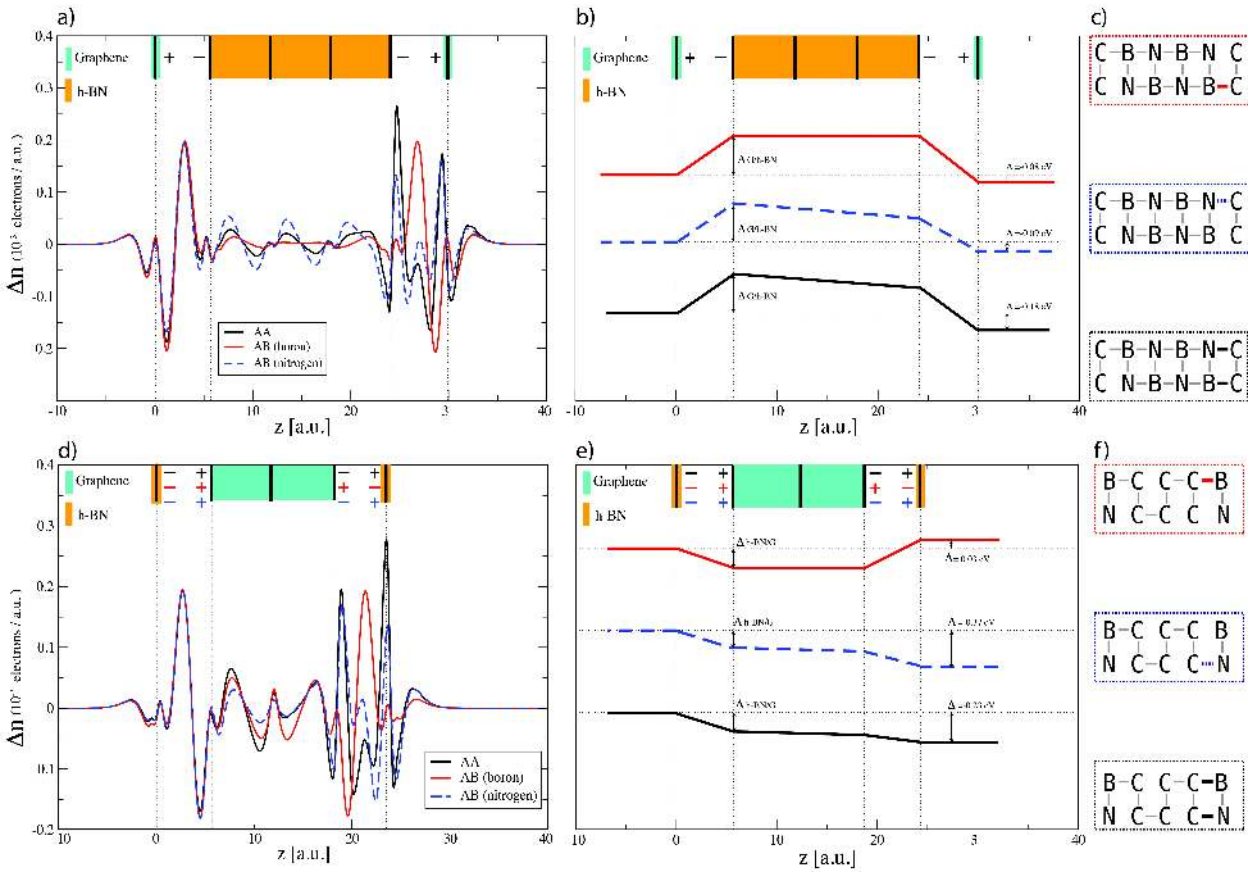

Fig. 4 Simulation model on h-BN and graphene stacking nanohybrids
(a) Plane integrated electronic density difference for a G |4 layers *h*-BN| G hetero stacked structure. The position of the top and the bottom layer of each substrate is indicated by a vertical dashed lines. We kept fixed the AB (boron) stacking at the first G/*h*-BN interface. We then slided the second graphene in order to produce three different stacking, the same that are sketched in the frame (c). A consistent use of colors both in the network representation and to plot and label the curves has been chosen to guide the eye (black for the AA stacking, red for the AB (boron) stacking and blue for the AB (nitrogen) stacking). It is possible to tune the distribution of electronic charge at the interface just changing the stacking as discussed in the manuscript.
(d) Plane integrated electronic density difference for a *h*-BN| trilayer Graphene| *h*-BN hetero stacked structure. The positions of the top and the bottom layer of each substrate is indicated by a

vertical dashed line. Keeping fixed the AB (boron) stacking at the first G/*h*-BN interface we slided the last *h*-BN layer generating three different stackings at the trilayer G/*h*-BN interface. We used the colors convention we explained rbefore. It is possible to change the sign of the dipole at the interface just changing the stacking (from AB (nitrogen) or AA to AB (boron)) as discussed in the manuscript.

(c) and (f) Network representation of the slab stacking. We define the following arrangements on the basis of the stacking nomenclature of graphite: AA (the carbon atoms of the graphene layer are on top of the nitrogen and boron of the *h*-BN layer), AB (a carbon atom is on top of the centre of the hexagon of the *h*-BN layer, while the other carbon is on top of either the nitrogen, AB (nitrogen) or the boron, AB (boron)). Similarly, the stacking arrangement of the 4 layers of *h*-BN is AA' (the boron and the nitrogen of one layer are respectively on top of nitrogen and boron of the layer below). The overlap position of two atoms belonging to two contiguous layers is marked by a grey segment. A missing connection between two atoms points at one atom positioned on the top of the centre of the hexagon below. In this way we end up with the following sequence in the frame (c): AB (boron) – AA'AA' – AB (boron) (red line), AB (boron) – AA'AA' – AB (nitrogen) (blue line) and AB (boron) – AA'AA' – AA (black line). In the frame (f) we find the following sequence of stackings: AB (boron) – ABC – AB (boron) (red line), AB (boron) – ABC – AB (nitrogen) (blue line) and AB (boron) – ABC – AA (dark line).

(b) Schematic representation of the electrostatic potential profile across the slab. The potential drop in the h-BN is proportional to the number of layers, and this influences the doping level of the graphene layer at the *h*-BN/G interface. Being the AB (boron) a quasi symmetric configuration the net doping effect is negligible. (The quasi symmetry comes from the fact that the two interfaces are the same but the two graphene layers are shifted one respect to the other. This is due to the AA' *h*-BN stacking and to the even number of layers composing the *h*-BN substrate. An odd number of layers and the same *h*-BN/G interface would have led to a symmetric configuration.) With the AB (nitrogen) and even more with the AA stacking the potential drop moves the electrostatic potential acting at the second *h*-BN/G to lower energies. This is connected with the gradient of the potential fall and consequently to the charge distribution at the interface.

(e) Schematic representation of the electrostatic potential profile across the slab. We use the stacking to change the sign of dipole, as discussed in the frame (d). The sign of dipole changes

the potential slope through the interface and consequently the electrostatic potential acting on the right h-BN layer is moved to higher energies or lower energies depending on the stacking, AB (boron) and AB (nitrogen) or AA respectively.

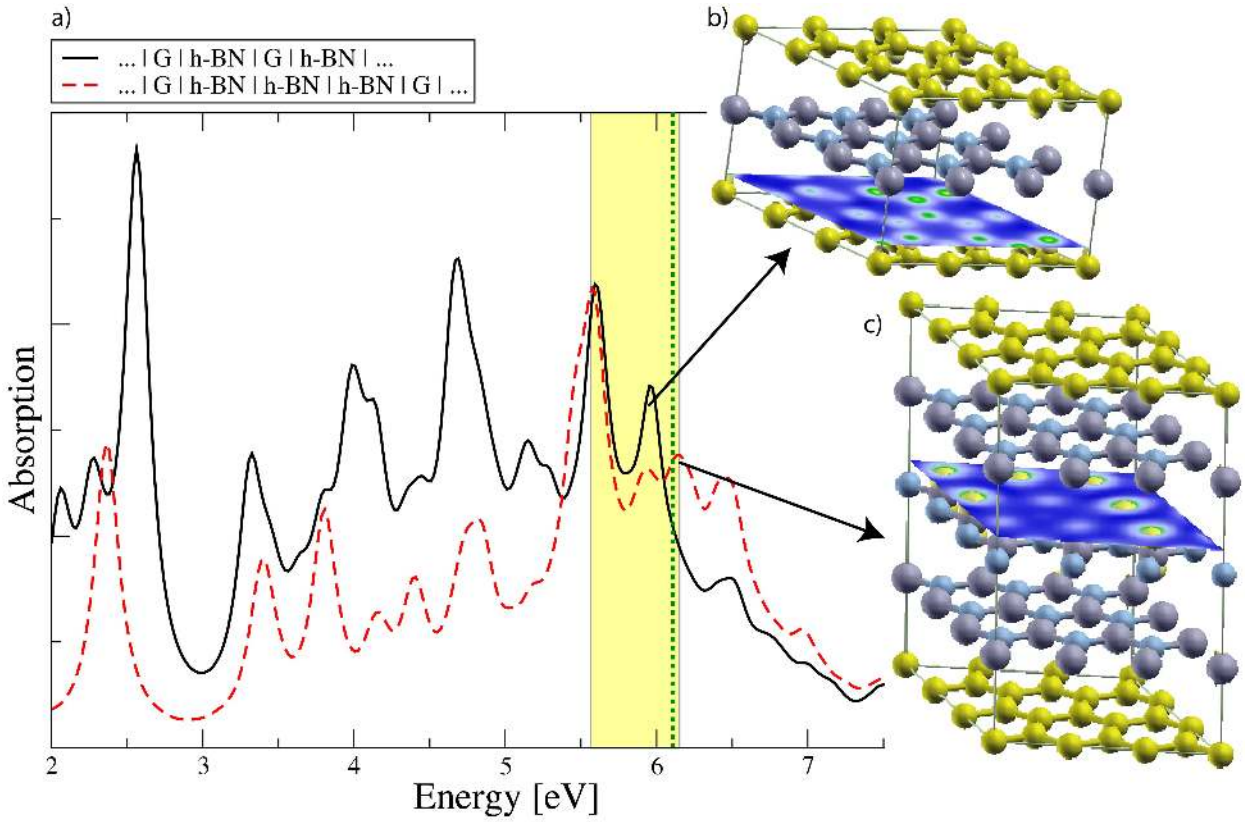

Fig. 5 Optical absorption spectra of a solid composed of alternated graphene and *h*-BN layers in the ratio 1:1 (solid dark line), and 1:3 (dashed red line). a)We show the results of the GW + Bethe-Salpeter approach, both lines are calculated with a broadening of 0.1 eV. The light polarization is parallel to the layers. The optical gap value position of the *h*-BN solid is marked by a green vertical dotted line[37]. The excitations of the 1:1 case (b) have a mixed nature, when the hole is localized on the *h*-BN layer the electron is on the graphene. In the 3:1 case (c) the excitations start to be localized on the *h*-BN layers, the energy region where this happens is inside the shadowed region.